ADVANCED MATERIALS

Supporting Information

for *Adv. Mater.*, DOI: 10.1002/adma.201303369

Highly-Efficient Capillary Photoelectrochemical Water Splitting Using Cellulose Nanofiber-Templated TiO_2 Photoanodes

Zhaodong Li, Chunhua Yao, Yanhao Yu, Zhiyong Cai, and Xudong Wang**

Supporting Information

for *Adv. Mater.*, DOI: 10.1002/adma.201303369

Highly-Efficient Capillary Photoelectrochemical Water Splitting Using Cellulose Nanofiber-Templated TiO_2 Photoanodes

Zhaodong Li, Chunhua Yao, Yanhao Yu, Zhiyong Cai, Xudong Wang **

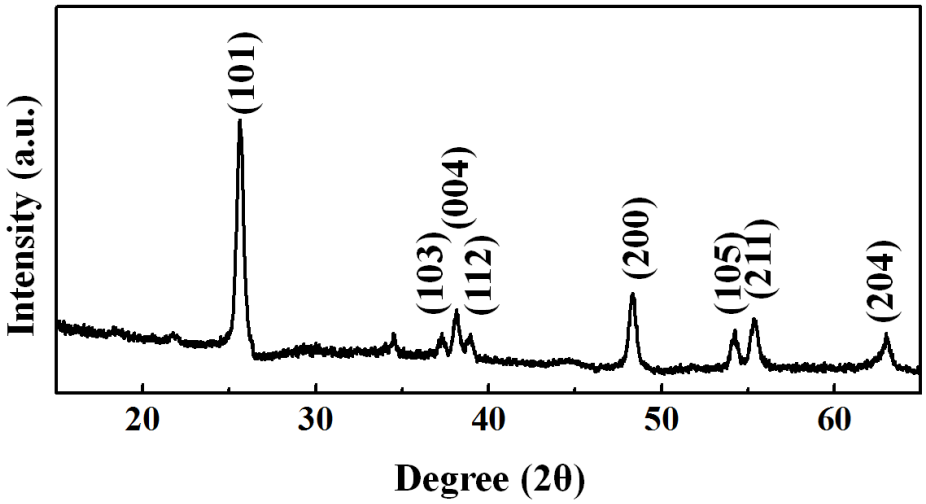

Figure S1. XRD spectrum of fibrous TiO_2 nanotubes after annealing, confirming its anatase phase.

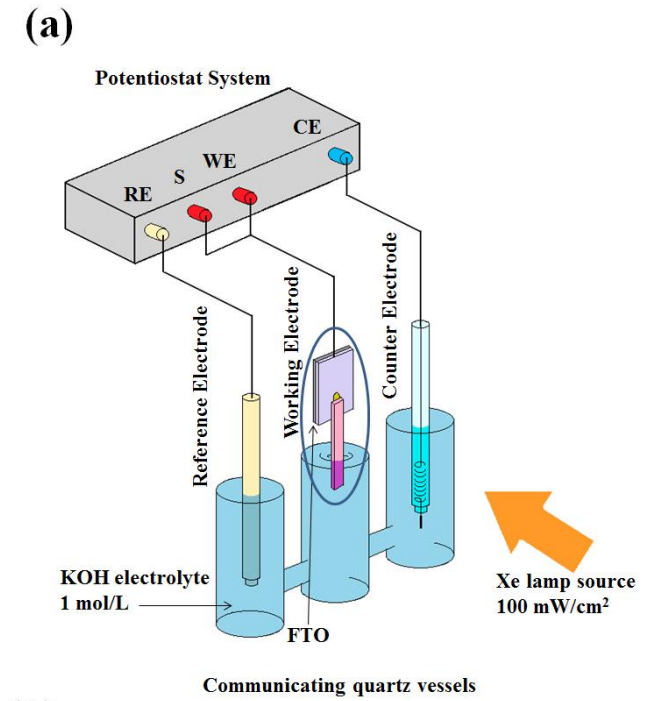

Figure S2. Schematic illustration (a) and a photo (b) of capillary PEC setup.

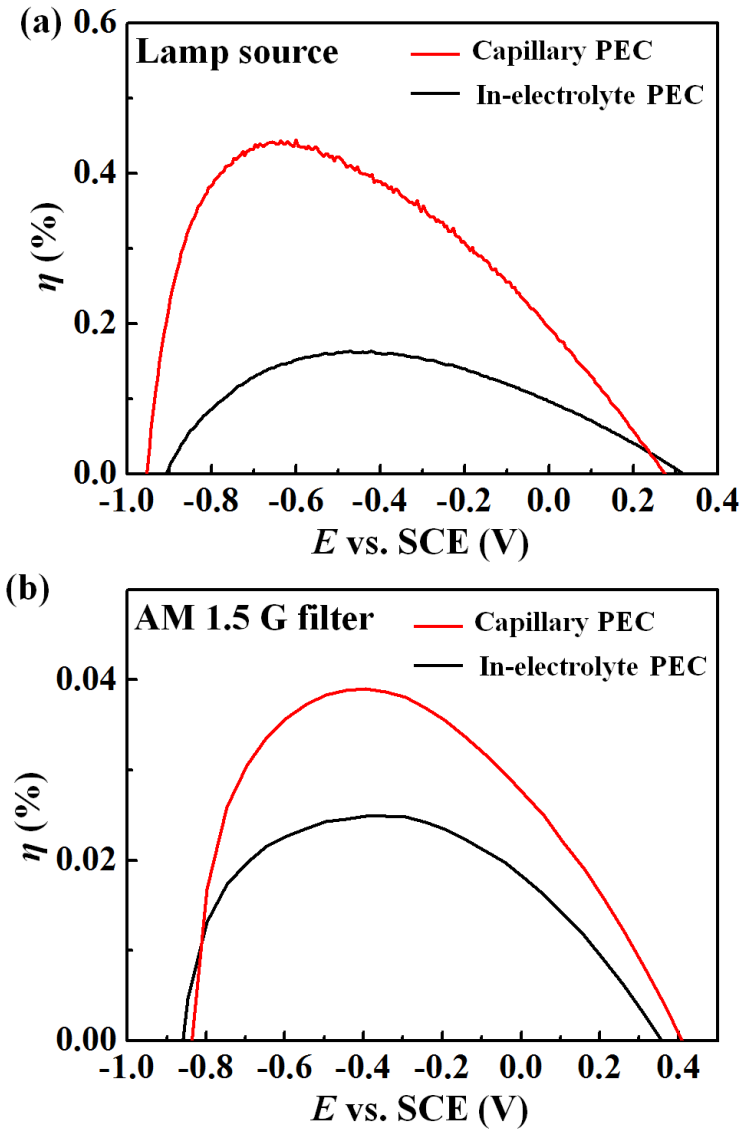

Figure S3. Calculated efficiencies versus bias voltages for capillary and in-electrolyte PEC setups using cellulose-templated TiO_2 photoanodes annealed in O_2 atmosphere. (a) Under Xe lamp illumination. (b) Under AM 1.5 G illumination.

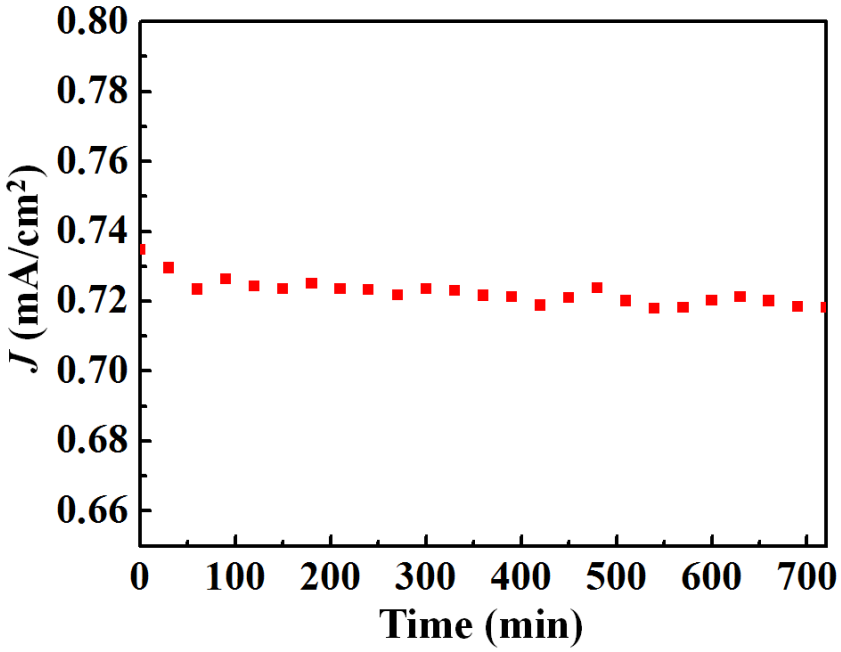

Figure S4. Stability test of capillary PEC setup under 0.3V (vs. SCE) bias for 12 hours.

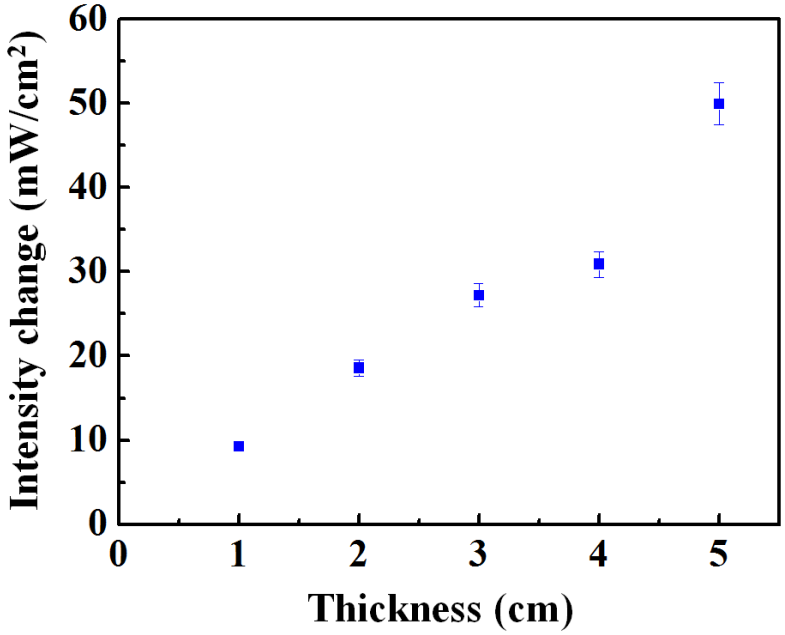

Figure S5. Illumination intensity decreases as a function of electrolyte (1M KOH) thickness that light passes through. The linear relation is consistent with the Beer–Lambert law.

S6: Analysis of pH-relationship

(1) Relationship between the Fermi level of the redox couple and their concentrations

$$E_{F,redox} = {}^{0}E_{redox} + kTln\left(\frac{[Red]}{[Ox]}\right)$$

where ${}^{0}E_{redox}$ is the standard redox potential of the redox couple.[1]

For $4OH^- \rightarrow 2H_2O + O_2 + 4e^-$

[Red] = [OH^-], [Ox] = [O_2] = P_{O_2}

At pH =14,

$$E^1_{F,redox} = {}^{0}E_{redox} + kTln(\frac{1}{P_{O_2}})$$

Also, [OH^-] = $10^{-14}/[H^+]$

At new pH value,

$$E^2_{F,redox} = {}^{0}E_{redox} + kTln(\frac{10^{-14}}{P_{O_2}[H^+]})$$

Thus, the potential change of the redox couple between new pH solution and pH=14 solution is:

$$\Delta\varphi_1 = E^2_{F,redox} - E^1_{F,redox} = \frac{kT}{lge} lg\left(\frac{10^{-14}}{[H^+]}\right) = \frac{kT}{lge}(pH - 14) = 0.059(pH - 14)$$

(2) Relationship between the Fermi level of the semiconductor and the number of accumulated holes

From interrupted *J-V* curve (black curves in the insets of Fig. 3) and the corresponding continuous *J-V* curve (red curves in the insets of Fig. 3), the area between them represents the number of accumulated holes at the semiconductor surface. Read data (V_0, J_0) at t_0 and (V_1, J_1) at t_1 on the black curve.

Based on the RC circuit model:

$$I(t) = I_0 e^{-\frac{t}{\tau_0}} = \frac{dQ(t)}{dt}$$

$Q_0 = CV_0$

$$I_0 = V_0/R = Q_0/RC$$

Thus, $$I(t) = (Q_0/RC)e^{-\frac{t}{\tau_0}}$$

Let $t=t_1-t_0$, where t can be achieved by $(V_1-V_0)/S$, S is the scan speed = 0.05V/s.

Put $(J_0, 0)$ and (J_1, t) into the equation to obtain the value of Q_0 (C cm^{-2})

For in-electrolyte PEC setup and capillary PEC setup, the average Q_0/e value were obtained as 8.24×10^{12}(cm^{-2}) and 3.43×10^{12}(cm^{-2}).

In our experiments, the thickness of the TiO_2 nanotube film was ~10 μm. Therefore, the concentrations of trapped holes were approximately 8.24×10^{15}(cm^{-3}) and 3.43×10^{15}(cm^{-3}) for in-electrolyte and capillary setups, respectively.

The current spikes diminish at higher potential as a larger proportion of holes have sufficient potential to oxidize water.[2] Previous research also revealed that the magnitude of the current spikes decreases with increasing positive bias. This effect was explained by bending of the favored band due to positive potentials.[3] Therefore, understanding the difference between the number of accumulated holes for the two PEC setups is equivalent to investigating the difference of band shifting using the following equations:

$$E_i - E_{f_1} = kTln(\frac{N_1}{N_i})$$

$$E_i - E_{f_2} = kTln(\frac{N_2}{N_i})$$

N_1 is the carrier concentration in TiO_2 photoanodes; $N_2 = N_1+\Delta N$, where ΔN (>0) is the change of hole concentration determined from J-V curves (ΔN~5×10^{15} cm^{-3}). Typically, for n-type TiO_2, N_1=~10^{17} (cm^{-3}). Thus,

$$\Delta\varphi_2 = E_{f_1} - E_{f_2} = kTln\left(\frac{N_2}{N_1}\right) = kTln\left(1+\frac{\Delta N}{N_1}\right)$$

(3) Relationship between pH and accumulated charges.

The water oxidation reaction occurs when the over potential between semiconductor and electrolyte is met. Assume the value of over potential does not change in our TiO_2 - KOH system and in the two PEC setups, the TiO_2 nanotube photoanodes did not change. Thus, the calculated potential difference for the semiconductor described in section 2 is actually the potential difference for KOH solution.

Let $\Delta\varphi_1 = \Delta\varphi_2$, we have:

$$0.059(pH - 14) = kTln\left(1 + \frac{\Delta N}{N_1}\right)$$

For N_1~10^{17}, ΔN~5×10^{15}, kT~0.025eV

Then, pH $\approx$ 14.02

To confirm the pH effect, PEC measurement was performed within an electrolyte with a pH value of 14.02 using the in-electrolyte setup. As shown in Figure S6, no initial current spikes were observed.

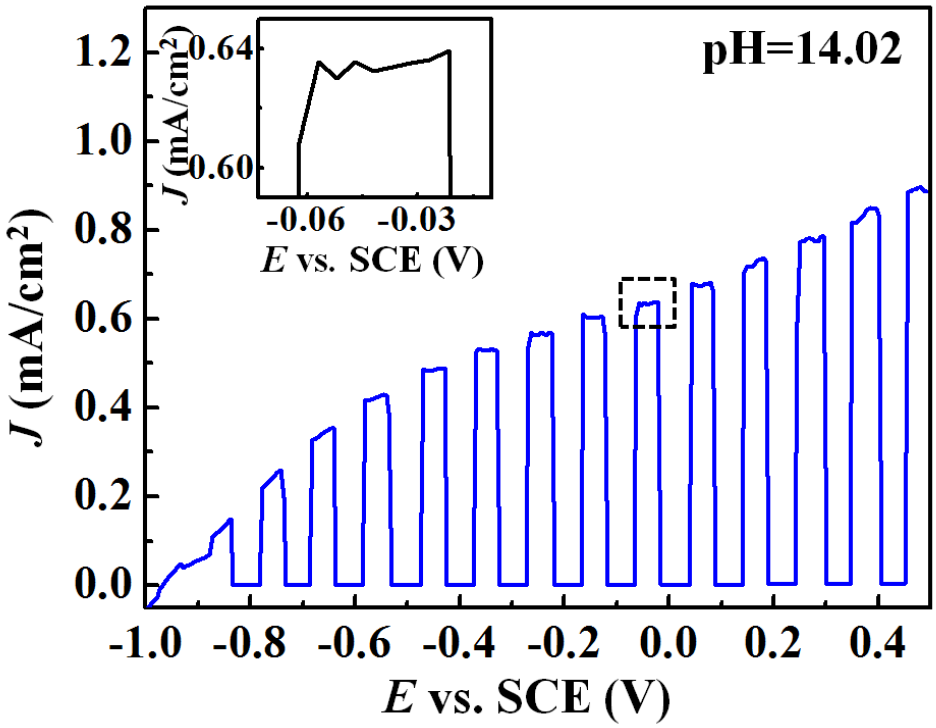

Figure S6. *J-V* characteristics of cellulose-templated TiO_2 photoanodes measured under interrupted illumination using in-electrolyte PEC setup, where the pH value of electrolyte was 14.02. Inset is enlarged top regions of one J_{ph} cycle showing the flatness of initial current.

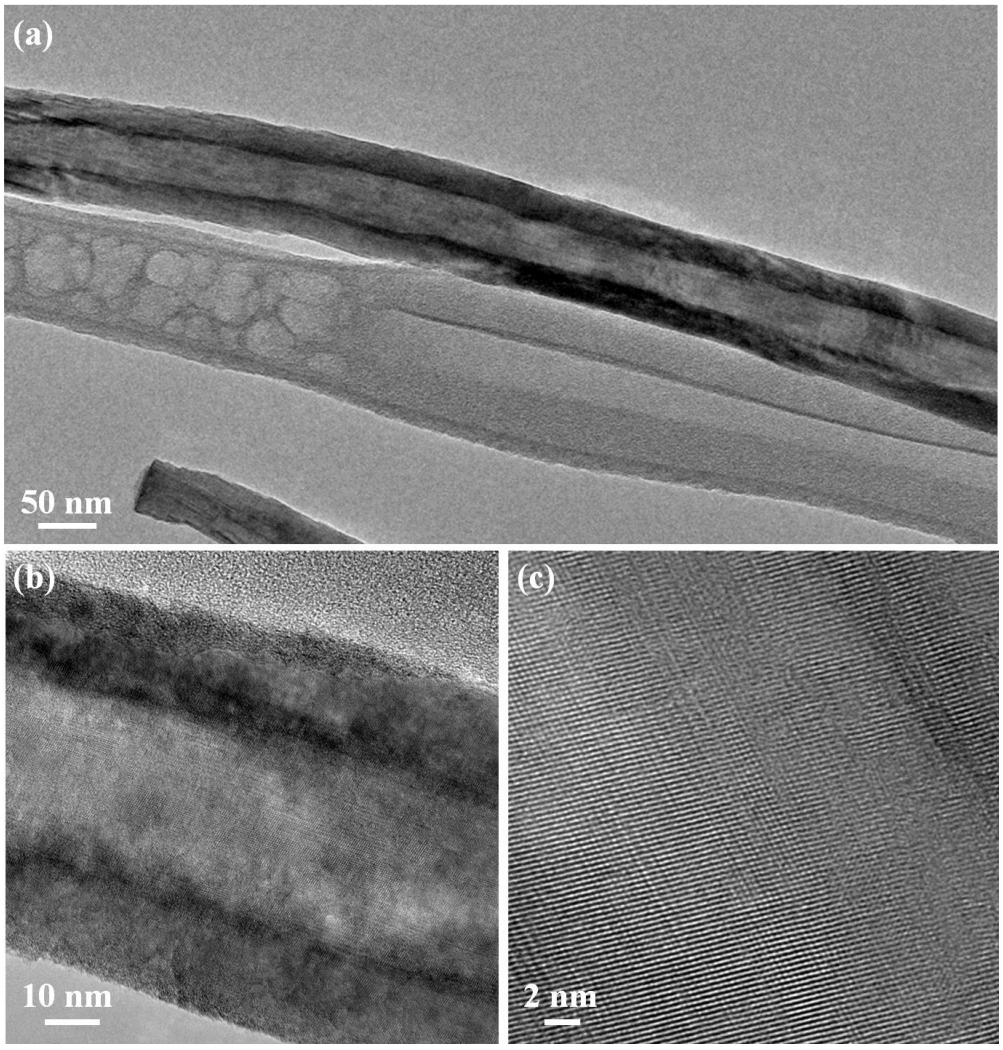

Figure S7. (a) TEM image of fibrous TiO_2 nanotubes obtained after 600 °C 24 hours annealing in vacuum. (b) TEM image showing TiO_2 wall with uniform thickness. (c) HRTEM image of TiO_2 wall showing good crystallinity.

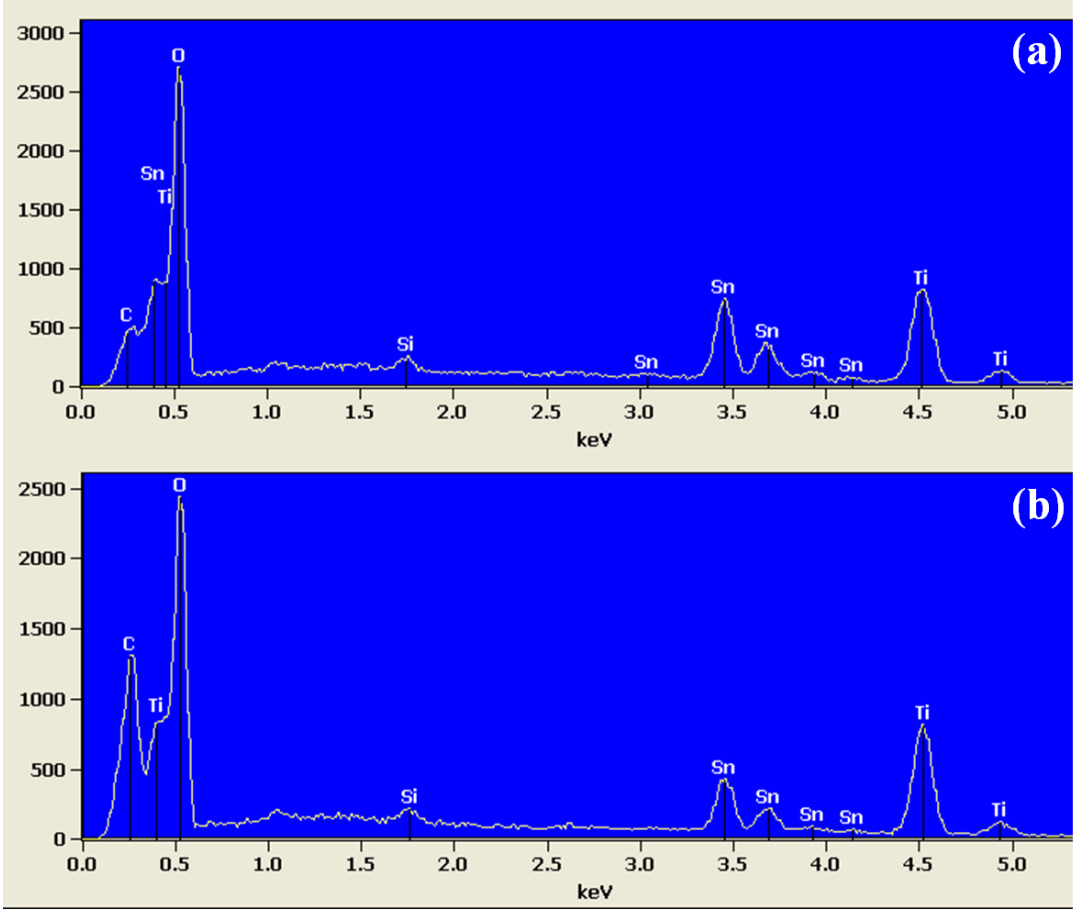

Figure S8. EDS spectra of fibrous TiO_2 nanotube samples after 600 ℃ annealing for 24 hours under the environment of O_2 atmosphere (a) vacuum (b). The observed average elemental content of carbon (atom %) was 5.713% for TiO_2 annealed in O_2 atmosphere; and 10.025% for TiO_2 annealed in vacuum. The "Si" peak and "Sn" peaks came from the FTO glass substrate.

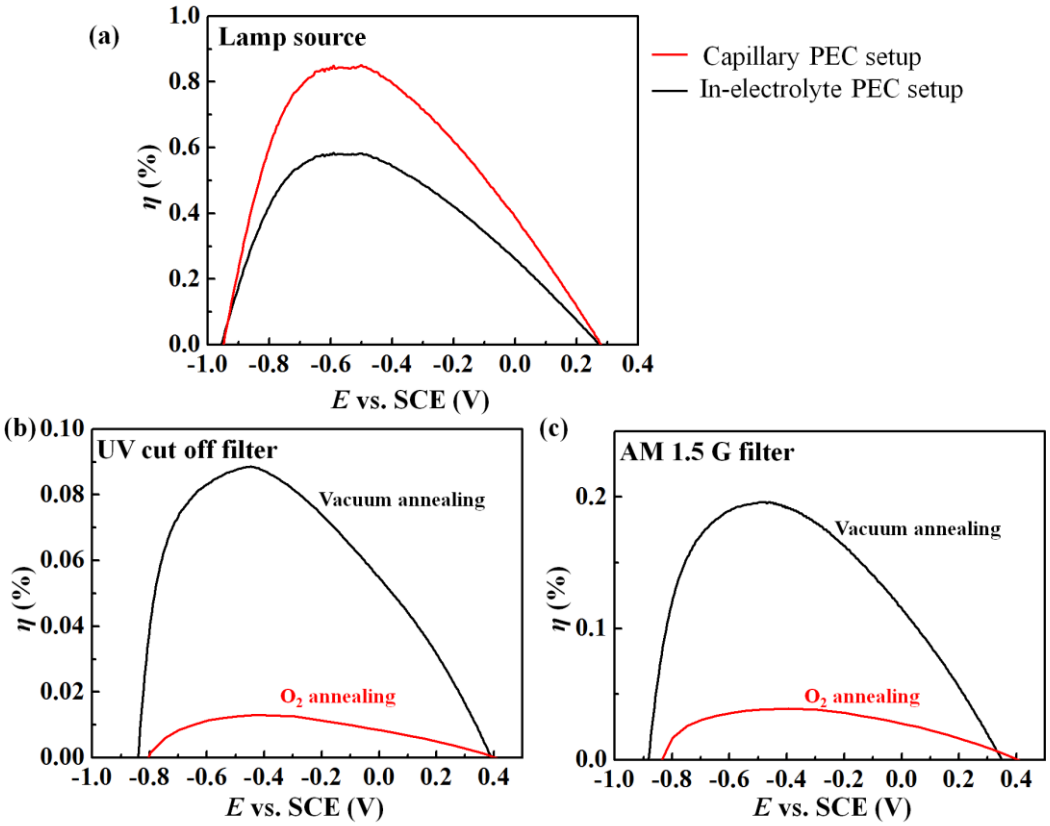

Figure S9. (a) Calculated efficiencies of "black" cellulose-templated TiO_2 photoanode measured using capillary and in-electrolyte PEC setups under Xe lamp illumination. (b, c) Calculated efficiencies of cellulose-templated TiO_2 photoanodes annealed in vacuum (black curves) and in oxygen (red curves) measured with UV cutoff filter (c) and AM 1.5 G filter (d). All the curves were measured using capillary PEC setup.

References:

[1] Arthur J. Nozik. PHOTOELECTRO CHEMISTR Y: APPLICATIONS TO SOLAR ENERGYCONVERSION. Ann. Rev. Phys. Chern. 1978. 29: 189-222.

[2] Florian Le Formal, Nicolas T_etreault, Maurin Cornuz, Thomas Moehl, Michael Grätzel and Kevin Sivula. Passivating surface states on water splitting hematite photoanodes with alumina overlayers. Chem. Sci., 2 (2011) 737–743.

[3] C. Sanchez, K.D. Sieber and G.A. Somorjai. The photoelectrochemistry of niobium doped α-Fe2O3, J. Electroanal. Chem., 252 (1988) 269-290